J. Fluid Mech. (2004), *vol.* 514, *pp.* 271–280.
DOI: 10.1017/S0022112004000291 Printed in the United Kingdom

On the coherent drag-reducing and turbulence-enhancing behaviour of polymers in wall flows

By YVES DUBIEF[1], CHRISTOPHER M. WHITE[2], VINCENT E. TERRAPON[2], ERIC S. G. SHAQFEH[2,3], PARVIZ MOIN[1,2] AND SANJIVA K. LELE[2,4]

[1]Center for Turbulence Research, [2]Mechanical Engineering Department, [3]Department of Chemical Engineering, [4]Department of Aeronautics and Astronautics, Stanford University, CA 94305, USA

(Received 15 December 2003 and in revised form 2 June 2004)

Numerical simulations of turbulent polymer solutions using the FENE-P model are used to characterize the action of polymers on turbulence in drag-reduced flows. The energetics of turbulence is investigated by correlating the work done by polymers on the flow with turbulent structures. Polymers are found to store and to release energy to the flow in a well-organized manner. The storage of energy occurs around near-wall vortices as has been anticipated for a long time. Quite unexpectedly, coherent release of energy is observed in the very near-wall region. Large fluctuations of polymer work are shown to re-energize decaying streamwise velocity fluctuations in high-speed streaks just above the viscous sublayer. These distinct behaviours are used to propose an autonomous regeneration cycle of polymer wall turbulence, in the spirit of Jiménez & Pinelli (1999).

1. Introduction

The addition of small amounts of long-chain polymer molecules to wall-bounded flows can lead to dramatic drag reduction. Although this phenomenon has been known for about fifty years, the action of the polymers and its effect on turbulent structures are still unclear. Detailed experiments have characterized two distinct regimes (Warholic, Massah & Hanratty 1999), referred to as low drag reduction (LDR) and high drag reduction (HDR). The first regime exhibits similar statistical trends to Newtonian flow: the log-law region of the mean velocity profile remains parallel to that of the Newtonian flow but its lower bound moves away from the wall and the upward shift of the log-region is a function of drag reduction, herein referred to as DR. Although streamwise fluctuations are increased and transverse ones are reduced, the shape of the r.m.s. velocity profiles is similar. At higher drag reductions, larger than about 40%, the flow enters the HDR regime for which the slope of the log-law is dramatically augmented and the Reynolds shear stress is small (Warholic *et al.* 1999; Ptasinski *et al.* 2003). The drag reduction is eventually bounded by a maximum drag reduction (MDR, Virk & Mickley 1970) which is a function of the Reynolds number.

In drag-reduced flows, a stress deficit is observed in the stress balance whose large magnitude at HDR has been interpreted as the necessary input of energy from the polymers to the flow for the sustenance of the asymptotic MDR turbulence (Warholic *et al.* 1999). Recently, numerical simulations have allowed the simultaneous study of velocity and polymer fields, giving the opportunity to relate turbulence and polymer

stress directly. Several explanations have been proposed for the mechanism of polymer drag reduction through such computations. Based on averaged budgets of kinetic and energy, Dimitropoulos *et al.* (2001) observed that streamwise enstrophy is inhibited by the extensional viscosity generated by polymers stretched by turbulence. Based on a similar argument, Ptasinski *et al.* (2003) related the damping of vortices to a shear sheltering effect occurring in the near-wall region which would effectively decouple the outer layer vortices from the inner layer. Neither paper proposes a mechanism for the injection of energy from polymers to turbulence. Min, Yoo & Choi (2003*a*) and Min *et al.* (2003*b*) analysed their simulation in terms of elastic energy, observing a significant transport of this energy from the viscous sublayer to the buffer layer and the log region. They derived a criterion for the onset of drag reduction based on the relaxation time and the time required for polymers to travel from the viscous sublayer to the buffer layer. These authors explain MDR by the release of energy into the buffer layer, which would be sufficient to sustain turbulence. All these studies have relied on the study of the time- and space-averaged statistics.

Near-wall vortices, critical to the production of wall friction (Kravchenko, Choi & Moin 1993), occupy a volume of about 10% of the buffer region in Newtonian flows and the streamwise vorticity fluctuations they generate in their core and immediate surroundings exceed the standard deviation of ω_x by a factor of 2 or more (Dubief & Delcayre 2000). Since ultra-dilute solutions of polymers are not expected to change significantly the properties of the flow, the effect of polymers can be assumed to be local and triggered by the most energetic turbulent structures. This assumption implies that the action of polymers is likely to be as intermittent as the near-wall vortices. Intermittent events are hidden by the averaging procedure and it seems therefore natural to find an approach which reveals the dynamics of these rare events.

The intermittency of polymers in turbulent flows is addressed here by identifying regions of the flow where polymers dampen or enhance turbulence. Viscoelastic direct numerical simulations, using the FENE-P model, provide the requisite information. After a brief presentation of the flow conditions and viscoelastic parameters, the contribution of polymer work to the instantaneous budget of energy of each velocity component is characterized in the near-wall region. Intermittency is captured by using joint probability functions and by focusing on the large and rare fluctuations of polymer work (defined in § 4). Finally, a model of drag-reduced near-wall turbulence is proposed based on the autonomous regeneration cycle of near-wall turbulence of Jiménez & Pinelli (1999).

2. Governing equations and numerical method

The formalism of the constitutive equations for viscoelastic flows typically includes the assumption of uniform concentration of the polymer solution, and the momentum equations thus become

$$\partial_t \tilde{u}_i = -\tilde{u}_j \partial_j \tilde{u}_i - \partial_i \tilde{p} + \frac{\beta}{Re} \partial_j \partial_j \tilde{u}_i + \underbrace{[(1-\beta)/Re] \partial_j \tilde{\tau}_{ij}}_{\tilde{f}_i}, \tag{2.1}$$

where β is the ratio of the solvent viscosity ν to the total viscosity and effectively controls the concentration of polymers. Hereafter, $\tilde{a}$ represents the instantaneous value of variable a which is the sum of its mean $\overline{\tilde{a}} = A$ and instantaneous fluctuations a. The flow investigated here is the channel flow, for which the Reynolds number is defined as $Re = U_c h/\nu$, based on the centreline velocity of a Poiseuille flow, U_c, and the channel half-width, h. Note the addition of an extra term, which will be hereafter

referred to as the *polymer body force*, $\tilde{f}_i$. The polymer stress tensor $\tilde{\tau}_{ij}$ in $\tilde{f}_i$ is obtained by solving the FENE-P (finite elastic non-linear extensible-Peterlin) equation,

$$\partial_t \tilde{c}_{ij} = \underbrace{-\tilde{u}_k \partial_k \tilde{c}_{ij}}_{\text{advection}} + \underbrace{\tilde{c}_{kj}\partial_k \tilde{u}_i + \tilde{c}_{ik}\partial_k \tilde{u}_j}_{\text{stretching}} \underbrace{- \frac{1}{We}\left(\frac{\tilde{c}_{ij}}{1-\tilde{c}_{kk}/L^2} - \delta_{ij}\right)}_{=\tilde{\tau}_{ij}:\text{relaxation}} + \kappa \mathrm{D}(\tilde{c}_{ij}), \qquad (2.2)$$

where the conformation tensor, $\tilde{c}_{ij}$, is the phase average of $q_i q_j$, q_i being the component of the end-to-end vector of each individual polymer which has a maximum dimensionless extensibility L. The Weissenberg number We is the ratio of the polymer relaxation time λ to the flow time scale, such that $We = \lambda U/h$. The numerical method is essentially that of Min *et al.* (2003*b*) modified to simulate very elastic and long polymer molecules and is described and validated in Dubief *et al.* (2004). In the present paper only a brief outline of the method is given. The momentum equations are solved on a staggered grid with second-order central finite differences. The divergence of the polymer stress (2.1) and the spatial derivatives of $\tilde{c}_{ij}$ are computed using a fourth-order compact scheme and a third-order upwind compact scheme, respectively. Time advancement of (2.1) and (2.2) is performed by the classical semi-implicit second-order Crank–Nicolson/third-order Runge–Kutta scheme. In the momentum equation, the Newtonian viscous stress is treated implicitly in the wall-normal direction. Equation (2.2) is solved with a new semi-implicit time scheme which ensures that the trace of the $\tilde{c}_{ij}$ remains upper bounded ($\tilde{c}_{kk} < L^2$). A local artificial viscosity (LAD), proposed by Min *et al.* (2003*b*), is necessary to ensure the stability of the advection term as well as a lower diffusive effect than a global dissipation as adopted in Dimitropoulos *et al.* (2001) and Ptasinski *et al.* (2003). The LAD is represented in (2.2) by $\kappa \mathrm{D}(\tilde{c}_{ij})$, where κ is non-zero only in regions where the conformation tensor loses its positive definiteness and the operator D is defined as $\Delta_k^2 \partial_k^2$, Δ_k being the local grid spacing in the k-direction. For the present simulations, κ is equal to 0.1. For further information regarding the impact of LAD on the flow, refer to Dubief *et al.* (2004).

Finally, as in any simulation involving dramatic reduction of drag, particular care with the dimensions of the computational domain is required. Here, simulations are performed in a channel flow, where periodic boundary conditions are enforced in the streamwise and spanwise directions (x and z, respectively) and no-slip is prescribed in the wall normal direction, y. The streamwise and spanwise dimensions are larger than for a typical Newtonian simulation due to the coarsening of near-wall structures as observed experimentally by White, Somandepalli & Mungal (2004). Their experiment shows that the streamwise coherence of the streaks could be increased by an order of magnitude of the Newtonian length scale $l^+ \sim 1000$, where the superscript $^+$ denotes normalization by inner scaling based on the kinematic viscosity ν and the friction velocity $u_\tau = \sqrt{\nu(\mathrm{d}U_x/\mathrm{d}y)_{wall}}$. In a preliminary parametric study for 60% drag reduction, streamwise correlations of velocity were indeed found to be small yet finite even for $L_x^+ = 6000$ based on the Newtonian friction velocity, while $L_z^+ = 1000$ proved to be sufficient. Decreasing L_x^+ to 4000 had a negligible impact on the magnitude of drag reduction, less that 5%, well within the convergence error of statistics, and this length was adopted for the present study. Note that reducing the domain size to $L_x^+ \times L_z^+ = 1000 \times 300$ leads to a drag reduction comparable to that of Maximum drag reduction, 72% instead of 60%. Periodic conditions in that case totally damp all the scales larger than the domain. Nevertheless, the turbulence was found to be self-sustained in a similar fashion to the minimal channel flow of Jiménez & Moin (1991) which contains only a pair of streaks and vortices. This point is further discussed in Dubief *et al.* (2004).

Line/symbol	L	$We_{\tau 0} = \lambda u_{\tau 0}^2/\nu$	$We = \lambda U/h$	β	DR
– – – –					0%
○	100	36	3	0.9	35%
●	60	84	7	0.9	47%
■	100	120	10	0.9	60%

TABLE 1. Polymer parameters used for the viscoelastic simulations. The Weissenberg number $We_{\tau 0}$ is normalized by the wall-shear stress for the Newtonian simulation (DR = 0%).

Simulations are performed at an intermediate Reynolds number, $Re_c = 7500$, or a bulk Reynolds number of $Re_M = 5000$. Conservation of the mass flow is imposed which gives $h^+ = hu_\tau/\nu = 300$. The resolution is $\Delta x^+ = 9$, $\Delta y^+ = 0.1$–5 and $\Delta z^+ = 6$, when normalized by the skin friction at DR = 0%. Statistics are collected over 300 to 400 convection times h/U, starting after the transient period.

3. A brief statistical description of drag-reduced flows

In the following, the simulations are referred to by the amount of drag reduction: DR = 35%, DR = 47% and DR = 60% (cf. table 1). As shown in table 1, the FENE-P model requires fairly high Weissenberg numbers to achieve HDR with long-chain polymers, while HDR has experimentally been measured for *We* ranging from unity to 100. This observation holds for all published simulations and using a FENE-P model. For this model, large stress can only be obtained when polymers are significantly stretched. In the two viscoelastic simulations discussed here, polymers are stretched to less than 50% of their maximum extension, with $c_{kk}/L^2 < 35\%$ on average for DR = 60%. In this regime of mild extension, internal modes may be expected to play an important role and are not represented in the FENE-P model. This argument and perhaps also the low Reynolds number are a reasonable explanation for the overestimation of drag-reducing We_τ. We shall not discuss this issue further, since our goal is to understand how (2.1) and (2.2) produce flows whose characteristics are qualitatively identical to polymer drag-reduced flows observed experimentally. Turbulence statistics are presented here to validate the present simulations and introduce the reader to the mean effect of polymers on turbulence.

As expected from experiments (Warholic *et al.* 1999), DR = 35% produces a velocity profile whose log region is only shifted upward, while DR = 47% and DR = 60% show significant changes in the slope of the log law (figure 1). Although we did not attempt to determine an accurate limiting value, the transition between LDR and HDR seems to be near 40% DR, in agreement with Warholic *et al.*'s measurements. The turbulent velocity fluctuations in the transverse directions exhibit a different behaviour than in the streamwise direction. The peak of u_x' (a' denotes the root mean square of a fluctuations) shifts away from the wall and its magnitude increases slowly compared to the Newtonian flow when normalized by u_τ. The wall-normal component u_y' follows an opposite trend; u_z' behaves as u_y' and consequently does not appear on the plot for clarity. In drag-reduced flow, the maximum of $u_x'^+$ is higher than or comparable with the DR = 0% case, as found in experiments (Warholic *et al.* 1999; Ptasinski *et al.* 2003; White *et al.* 2004). The strong reduction of the transverse fluctuations suggests that polymers target preferentially the vortices, as they produce significant fluctuations of u_y and u_z.

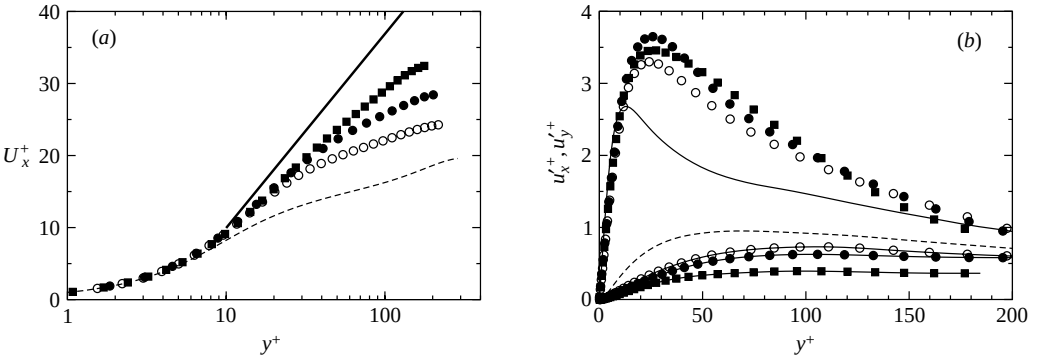

FIGURE 1. (*a*) Mean velocity profiles scaled with inner variables. ——— : MDR asymptote, $U^+ = 11.7 \ln y^+ - 17$. Symbols and lines are defined in table 1. (*b*) RMS of velocity fluctuations scaled with inner variables. Newtonian simulation (DR = 0%): ———, $u_x'^+$; – – – –, $u_y'^+$. For the viscoelastic simulations, symbols are defined in table 1, $u_x'^+$ is denoted by symbols only; $u_y'^+$ is indicated by symbols connected by ———.

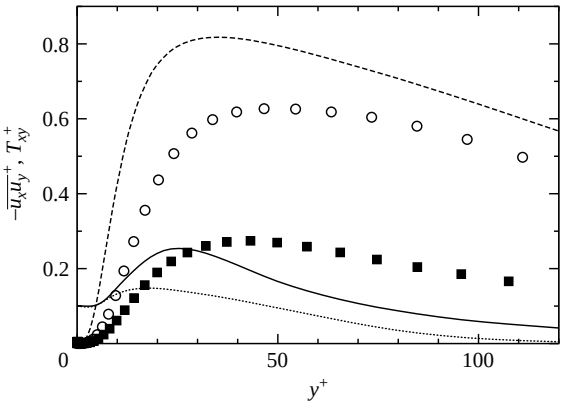

FIGURE 2. Reynolds shear stress (– – – –, ○ and ■ as in table 1) and polymer stress (·····, DR = 35%; ———, DR = 60%) normalized by u_τ and ν. DR = 47% is not plotted for clarity.

The balance of shear stress,

$$-\overline{u_x u_y}^+ - \left(1 - \frac{y^+}{h^+}\right) + \beta \frac{\mathrm{d}U_x^+}{\mathrm{d}y^+} + (1-\beta) T_{xy}^+ = 0, \tag{3.1}$$

contains significant information on the mechanism of polymer interaction with the mean flow. In (3.1), T_{xy} is the average of $\tilde{\tau}_{xy}$. As indicated in figure 2, the Reynolds shear stress is reduced with increasing drag reduction. For DR = 60%, $-\overline{u_x u_y}^+$ is approximately a third of its magnitude in the Newtonian case. Conversely, the polymer stress increases with increasing drag reduction. At DR = 60%, its near-wall contribution to (3.1) has the same magnitude as the Reynolds shear stress, thus showing that polymers have a significant mean effect in the mechanism of HDR flows, as argued by Warholic *et al.* (1999).

4. The role and intermittency of polymer work

As suggested in § 1, a factor that has been overlooked in the existing literature is the intermittency of the polymer action on turbulence. In wall flows, energetic structures

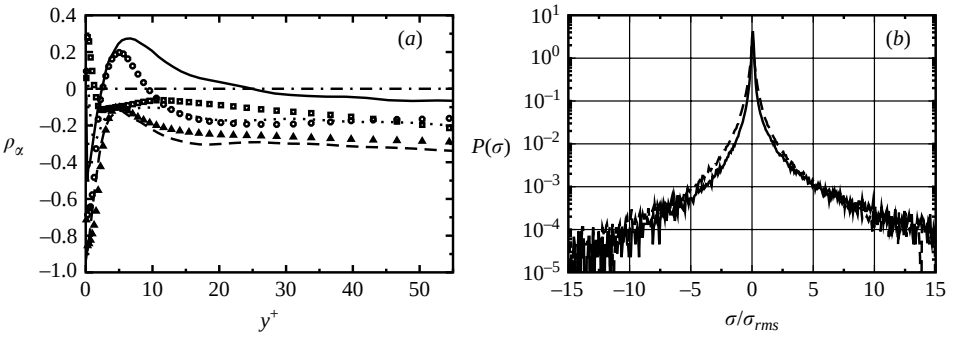

FIGURE 3. (*a*) Correlation of velocity–viscoelastic stress equation (4.2) in the streamwise (———, ○), wall-normal (·····, □) and spanwise (– – – –, △) directions. Lines: DR = 60%; Symbols: DR = 35%. (*b*) Probability density functions of E_x (———), A_x (– – – –) at $y^+ = 5$ for $DR = 60\%$.

close to the wall are only an order of magnitude larger than the smallest turbulent scale. These structures are the quasi-streamwise vortices which occupy less than 10% of the volume of the buffer layer (Dubief & Delcayre 2000), yet they are essential to momentum exchanges between outer and inner regions in the flow and are responsible for turbulent skin friction drag (Kravchenko *et al.* 1993). If polymers inhibit only vortices as suggested by the reduction of enstrophy observed by Dimitropoulos *et al.* (2001), polymer dynamics has to be intermittent.

To characterize the energy which is stored or released by polymers from each fluctuating velocity component, we consider the Reynolds stress equation (where summation does not apply to the subscript α)

$$\frac{1}{2}\partial_t u_\alpha^2 = \underbrace{(-u_\alpha \partial_j u_\alpha u_j)}_{A_\alpha} + \underbrace{(-u_\alpha \partial_\alpha) p}_{P_\alpha} + \underbrace{(\beta/Re) u_\alpha \partial_j \partial_j u_\alpha}_{V_\alpha} + \underbrace{[(1-\beta)/Re] u_\alpha \partial_j \tau_{\alpha j}}_{E_\alpha} . \quad (4.1)$$

The relation between polymers and turbulence enters through the *polymer work* E_α, the product of the velocity and polymer body force, which could dampen ($E_\alpha < 0$) or enhance ($E_\alpha > 0$) the energy carried by velocity fluctuations u_α. The other terms denote work by advection A_α, pressure redistribution P_α and viscous stress V_α; the sum of these terms will be later referred as to Newtonian work.

Figure 3(*a*) shows the evolution of the correlation between velocity and polymer body force,

$$\rho_\alpha = \frac{\overline{u_\alpha f_\alpha}}{u'_\alpha f'_\alpha} = \frac{\overline{E_\alpha}}{u'_\alpha f'_\alpha} \quad (4.2)$$

throughout the near-wall region for LDR and HDR. The correlation also provides an average measure of the polymer work. If the correlation is positive (negative), the body force f_α has the tendency to increase (decrease) the fluctuation u_α, which is equivalent to positive (negative) work. Very close to the wall, most of the wall-normal velocity fluctuations are increased while almost all the spanwise ones are dampened by polymers. Since u_y velocity fluctuations are extremely weak in this region (see figure 1*b*), the impact of an increase on turbulence is negligible, as it will be discussed in § 5. In the viscous sublayer, streamwise velocity fluctuations are dampened by polymers on average. However, in a region that begins on the upper edge of the viscous sublayer ($y^+ \simeq 3$–5) and whose width grows with increasing DR, u_x is enhanced on average by the polymer body force. By numerically forcing $f_y = f_z = 0$,

Dubief *et al.* (2004) showed that f_x alone has the effect of increasing drag and therefore turbulence, in spite of its turbulence damping property observed in the rest of the channel. Figure 3(*a*) suggests that this increase may arise from this region of positive ρ_x, also observed for uncoupled simulations ($\beta = 1$, not shown here). The qualitative behaviour of ρ_α shows very little dependence on the regime of drag reduction, LDR or HDR. Quantitatively, correlations just become stronger with increasing DR. The anti-correlation of velocity and polymer body force has also been reported by Stone, Waleffe & Graham (2001) and De Angelis, Casciola & Piva (2002) for LDR flows.

Figure 3(*b*) shows probability density functions (p.d.f.) of the different work terms in (4.1) for DR = 60% at $y^+ = 5$ (streamwise momentum). The stretched exponential tails of the p.d.f.s identify a strong intermittent behaviour of the structures producing large fluctuations of A_α and E_α; as the shape of V_α and P_α is similar, these are not shown for clarity. The p.d.f. of E_x is nearly symmetric for $P(E_x) > 10^{-3}$. Below this value, the p.d.f. shows an obvious positive skewness. Rare events producing large positive polymer fluctuations are therefore more probable than ones generating negative work of the same magnitude. It should be noted that all p.d.f.s of E_α show the same type of exponential tails, skewed in the negative side for $y^+ > 25$ (not shown here).

In figure 4, joint probability functions are used to illustrate the interesting correlations between large fluctuations of polymer work and turbulent structures. Each variable plotted here is normalized by its standard deviation and only the data at HDR are shown for clarity. We should point out that all the characteristics of the joint p.d.f.s presented here are identical at LDR, implying that the turbulence/polymers interaction is independent of the regime of drag reduction.

The most striking feature of polymer work is in the region where the correlation velocity/polymer body force ρ_x is positive (Figures. 4*a–d*). Large fluctuations of polymer work are exclusively contained in regions of positive streamwise velocity fluctuations (Figure 4*a*, solid contours). The magnitude of these fluctuations, above 3 times the standard deviation, corresponds to roughly 10% of the centreline mean velocity which is the typical velocity scale in high-speed streaks. In Newtonian channel flows, high-speed streaks receive a large contribution from downwash flows generated by the overlying vortices. However, as discussed earlier, these vortices are intermittent. Therefore the coherence inside high-speed streaks, which are typically longer than quasi-streamwise vortices, exceeds the duration of downwash flows. Figure 4(*a*) (dashed contours) shows that downwash, as well as upwash, flows(large fluctuations of u_y) produce negligible polymer work, while the largest positive fluctuations of E_x occur for near-zero fluctuations of wall-normal velocity. Figure 4(*a*) therefore indicates that the release of energy occurs after polymers are swept in this region around $y^+ \sim 5$ through downwashes or before they are ejected away from the wall by an upwash. Comparing Newtonian work ($N_x = A_x + P_x + V_x$) to polymer work at HDR reveals that large positive polymer work is triggered in regions where Newtonian turbulence would have a natural tendency, through viscosity mostly, to decrease the energy of streamwise velocity fluctuations (Figure 4*b*, dashed contours). Yet the net growth rate of energy ($\frac{1}{2}\partial_t u_x^2$) is positive in these regions. The importance of this injection of energy into the flow has been assessed in a numerical experiment reported in Dubief *et al.* (2004). The numerical cancellation of f_x in (2.1) for $y^+ < 20$ leads to full relaminarization of the flow, demonstrating that the positive fluctuations of E_x play a crucial role in the self-sustained mechanism of near-wall turbulence at HDR.

The turbulent-drag-reducing property of polymer flows is observed in the buffer and log regions where polymer work is mostly negative (see figure 3*a*). As discussed earlier, polymers dampen vortices via f_y and f_z. Figure 4(*c*,*d*) represents the distribution of

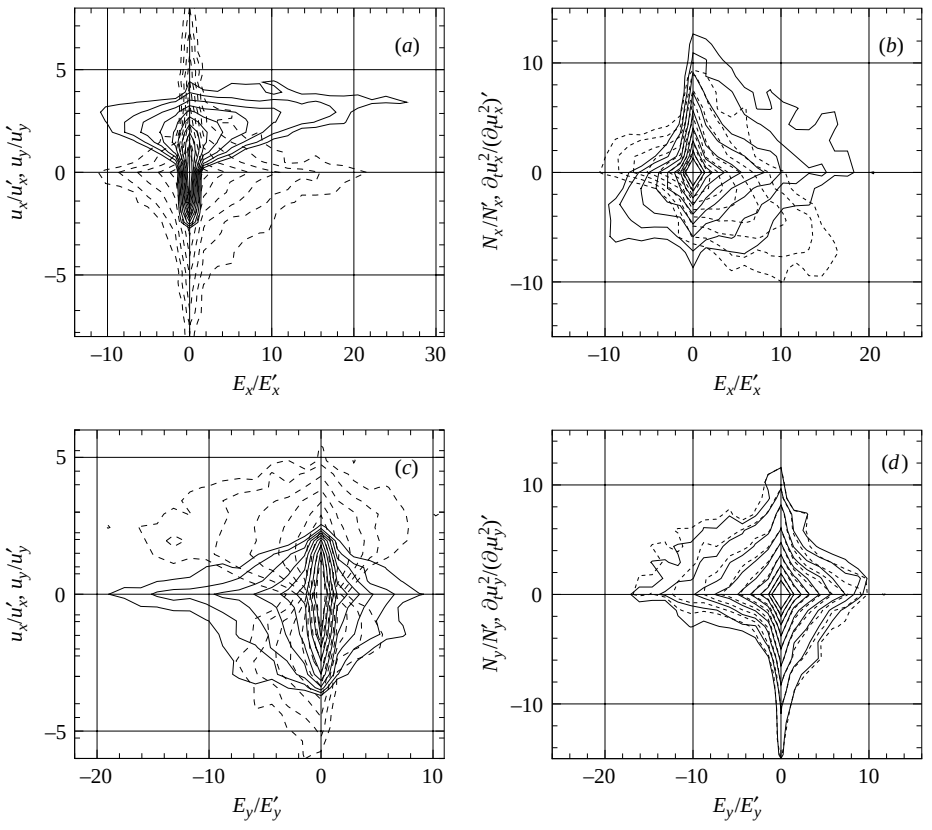

FIGURE 4. Joint probability density functions of polymer work *vs.* other relevant quantities. For each quantity, fluctuations are normalized by the respective standard deviation. Only data at DR = 60% are shown. (*a*) E_x *vs.* u_x (———) and u_y (– – – –) at $y^+ = 5$. (*b*) E_x *vs.* $N_x = A_x + P_x + V_x$ (– – – –) and $\frac{1}{2}\partial_t u_x^2$ (———) at $y^+ = 5$. (*c*) E_y *vs.* u_x (———) and u_y (– – – –) at $y^+ = 50$. (*d*) E_y *vs.* $N_y = A_y + P_y + V_y$ (– – – –) and $\frac{1}{2}\partial_t u_y^2$ (———) at $y^+ = 50$.

E_y at $y^+ = 50$, which shows strong negative skewness. Extraction of turbulent energy by polymers predominantly occurs in upwash flows, i.e. ($u_x < 0, u_y > 0$) (Fig. 4*c*) but also takes place in downwash flows ($u_x > 0, u_y < 0$). Large negative fluctuations of E_y are observed in regions of positive growth rate of u_y^2 (Figure 4*d*, solid contours) where polymer work opposes Newtonian work (figure 4*d*, dashed contours). Unlike the injection of energy in the streamwise direction at $y^+ = 5$, the extraction of energy by the polymers from the flow does not reverse the growth rate of u_y^2.

5. Mechanism of drag-reduced wall turbulence

The joint p.d.f.s presented in figure 4(*a*,*b*) show how polymers enhance the streamwise momentum in high-speed streaks located around $y^+ = 5$. Polymers are allowed to coil in these regions due to the reduction of turbulent kinetic energy by viscous dissipation as shown in figure 4(*b*). Extraction of energy from near-wall vortices by polymers occur as polymers are pulled around the vortices, either by upwash or downwash flows. Using Brownian dynamics simulations, Terrapon *et al.* (2004) showed that polymers experience significant straining around vortices, leading to large stretching. The importance of each transfer of energy for the self-sustained turbulence

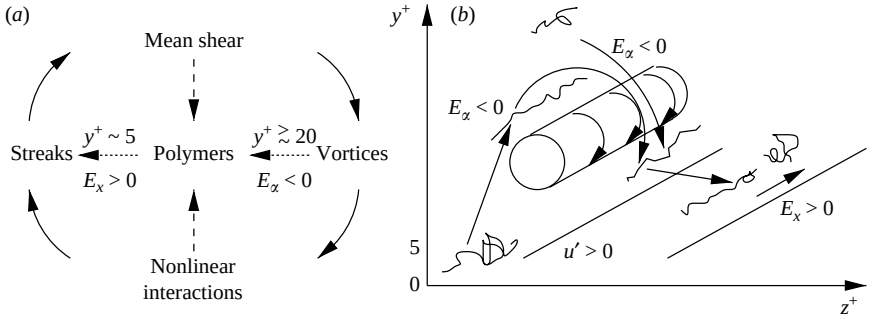

FIGURE 5. (*a*) Sketch of the cycle of wall turbulence regeneration with energy transfer from the polymers to the flow and vice versa, ····· denotes the action of polymers on turbulence, – – – – the main actions of stretching. (*b*) Vortex pumping fluid from the near-wall region and creating turbulence-damping polymer work and re-injecting stretched polymers into the near-wall region, thereby generating turbulence-enhancing polymer work.

in drag-reduced flows has been established by simple numerical experiments reported in Dubief *et al.* (2004).

Based on these results, we propose to include the effects of polymers in the autonomous regeneration cycle put forward by Jiménez & Pinelli (1999). This cycle, shown in figure 5, explains how wall turbulence is self-sustained through mean shear, nonlinear interactions, near-wall vortices and streaks, in the Newtonian case. Polymers fit at the centre of this cycle by extracting energy from the vortices and releasing energy in the streaks. The stretching of polymers is governed by the mean shear and nonlinear interactions as shown in Terrapon *et al.* (2004). This simple mechanism appears to apply to LDR and HDR regimes, and it should apply to any regime where streaks and vortices are present. Figure 5 also contains a sketch of the different actions of polymers around a vortex. Only the most dramatic phenomena, vortex damping and near-wall high-speed streaks enhancement are highlighted.

The phenomenology of the model in figure 5 shares many similarities with the different models proposed by previous efforts on the subject. It contains the damping of near-wall vortices discussed by Dimitropoulos *et al.* (2001), Stone *et al.* (2001), Min *et al.* (2003*b*) and Ptasinski *et al.* (2003). The originality of the model resides in the characterization of the drag-reducing and turbulence-enhancing effects of polymers. Our data indicate that the turbulence-enhancing effects is confined in the near-wall region and affects predominantly the streamwise velocity fluctuations. This analysis which comes from the study of small-scale quantities such as polymer work, differs from the interpretation of Min *et al.* (2003*a*) of the behaviour of elastic energy which is a larger scale quantity than polymer body force and gives the impression that elastic energy is released in the buffer and log layers.

6. Conclusion

Simulations of high drag reduction by a constitutive polymer model, FENE-P, have been presented. Statistical results reproduce the main features observed experimentally and in other numerical studies (Ptasinski *et al.* 2003; Min *et al.* 2003*a*). The bulk of this work consists of the characterization of the action of polymers on turbulent structures. This is achieved by studying the intermittent behaviour of $E_\alpha = [(1-\beta)/Re]u_\alpha \partial_k \tau_{\alpha k}$ through which polymers can dampen or enhance turbulence.

The drag-reducing and turbulence-enhancing properties of polymers are closely related to coherent turbulent structures. Polymers dampen near-wall vortices but also

enhance streamwise kinetic energy in near-wall streaks. The net balance of these two opposite actions leads to a self-sustained drag-reduced turbulent flow. The study of polymer work characterizes where polymers are most likely to release energy into the streaks. The phenomenon are related to regions where the streamwise kinetic energy u_x^2 would actually decrease in the absence of polymers. The release of energy in this region, which counteracts the viscous effects, occurs after polymers have resided in the streak but not when they have been transported from the buffer region to the streak through downwash flows initiated by vortices. Turbulence damping takes place in flows generated by vortices, therefore upwash and downwash flows occur around vortices with a preference for the upwash events, due to the pre-stretching caused by the higher shear close to the wall. This mechanism of polymer drag reduction is presented as a modified auto-regeneration cycle of wall turbulence.

The support of DARPA and its project manager, Dr. Lisa Porter, are gratefully acknowledged. This work is sponsored by Defense Advanced Research Projects Agency, Advanced Technology Office, Friction Drag Reduction Program, DARPA order: K042/31, K042/13, N115/00. Issued by DARPA/CMO, Contract No.: MDA972-01-C-0041.

REFERENCES

De Angelis, E., Casciola, C. M. & Piva, R. 2002 DNS of wall turbulence: dilute polymers and self-sustaining mechanisms. *Computers Fluids* **31**, 495–507.

Dimitropoulos, C. D., Sureshkumar, R., Beris, A. N. & Handler, R. A. 2001 Budget if reynolds stress, kinetic energy and streamwise enstrohpy in viscoelastic turbulent channel flow. *Phys. Fluids* **13**, 1016–1027.

Dubief, Y. & Delcayre, F. 2000 On coherent-vortex identification in turbulence. *J. Turbulence* **1** (011).

Dubief, Y., Terrapon, V. E., White, C. M., Shaqfeh, E. S. G., Moin, P. & Lele, S. K. 2004 New answers on the interaction between polymers and vortices in in turbulent flows. *Flow, Turbulence and Combustion* (to appear).

Jiménez, J. & Moin, P. 1991 The minimal flow unit in near-wall turbulence. *J. Fluid Mech.* **225**, 213–240.

Jiménez, J. & Pinelli, A. 1999 The autonomous cycle of near-wall turbulence. *J. Fluid Mech.* **389**, 335–359.

Kravchenko, A. G., Choi, H. & Moin, P. 1993 On the relation of near-wall streamwise vortices to wall skin friction in turbulent boundary layers. *Phys. Fluids* A **5**, 3307–3309.

Min, T., Yoo, J. Y. & Choi, H. 2003*a* Maximum drag reduction in a turbulent channel flow by polymer additives. *J. Fluid Mech.* **492**, 91–100.

Min, T., Yoo, J. Y., Choi, H. & Joseph, D. D. 2003*b* Drag reduction by polymer additives in a turbulent channel flow. *J. Fluid Mech.* **486**, 213–238.

Ptasinski, P. K., Boersma, B. J., Nieuwstadt, F. T. M., Hulsen, M. A., Van den Brule, B. H. A. A. & Hunt, J. C. R. 2003 Turbulent channel flow near maximum drag reduction: simulations, experiments and mechanisms. *J. Fluid Mech.* **490**, 251–291.

Stone, P. A., Waleffe, F. & Graham, M. D. 2001 Toward a structural understanding of turbulent drag reduction: nonlinear coherent states in viscoelastic shear flows. *Phys. Rev. Lett.* **89**, 208301.

Terrapon, V. E., Dubief, Y., Moin, P., Shaqfeh, E. S. G. & Lele, S. K. 2004 Simulated polymer stretch in a turbulent flow using Brownian dynamics. *J. Fluid Mech.* **504**, 61–71.

Virk, P. S. & Mickley, H. S. 1970 The ultimate asymptote and mean flow structures in Tom's phenomenon. *Trans. ASME E: J. Appl. Mech.* **37**, 488–493.

Warholic, M. D., Massah, H. & Hanratty, T. J. 1999 Influence of drag-reducing polymers on turbulence: effects of Reynolds number, concentration and mixing. *Exps. Fluids* **27**, 461–472.

White, C. M., Somandepalli, V. S. R. & Mungal, M. G. 2004 The turbulence structure of drag reduced boundary layer flow. *Exps. Fluids* **36**, 62–69.